

Chemical Understanding of Carbide Cluster Metallofullerenes: A Case Study on $\text{Sc}_2\text{C}_2@C_{2\nu}(5)-C_{80}$ with Complete X-ray Crystallographic Characterizations

Hiroki Kurihara,[†] Xing Lu,[†] Yuko Iiduka,[†] Hidefumi Nikawa,[†] Naomi Mizorogi,[†] Zdenek Slanina,[†] Takahiro Tsuchiya,[†] Shigeru Nagase,^{*,§} and Takeshi Akasaka^{*,†}

[†]Life Science Center for Tsukuba Advanced Research Alliance, University of Tsukuba, Tsukuba, Ibaraki 305-8577, Japan

[§]Department of Theoretical and Computational Molecular Science, Institute for Molecular Science, Okazaki, Aichi 444-8585, Japan

Supporting Information

ABSTRACT: Little is known about the chemical properties of carbide cluster metallofullerenes (CCMFs). Here we report the photochemical reaction of a newly assigned CCMF $\text{Sc}_2\text{C}_2@C_{2\nu}(5)-C_{80}$ with 2-adamantane-2,3-[3H]-diazirine (AdN_2 , **1**), which provides a carbene reagent under irradiation. Five monoadduct isomers (**2a–2e**), with respective abundances of 20%, 40%, 25%, 5%, and 10%, were isolated and characterized with a combination of experimental techniques including unambiguous single-crystal X-ray crystallography. Results show that the two Sc atoms of the bent Sc_2C_2 cluster tend to move in most cases, whereas the C_2 -unit is almost fixed. Accordingly, it is difficult to explain the addition patterns by considering the strain and charge density on the cage with a fixed cluster, and thus a moving cluster may account for the addition patterns. These results show that the situation of CCMFs is more complicated than those in other metallofullerenes. Furthermore, a thermal isomerization process from **2b** to **2c** was observed, confirming that the most abundant isomer **2b** is a kinetically favored adduct. Finally, it is revealed that the electronic and electrochemical properties of pristine $\text{Sc}_2\text{C}_2@C_{2\nu}(5)-C_{80}$ have been markedly altered by exohedral modification.

INTRODUCTION

Investigations of new carbon materials have been expanding rapidly in depth and scope during recent years because of their promising applications resulting from their novel structures and fantastic properties.¹ As the only molecular allotrope of elemental carbon, fullerenes have attracted great attention because of their unique closed-cage structures and interesting properties, giving potential applications in many fields, such as biomedicine and photovoltaics.²

To realize the applications of fullerenes, it is necessary to attach different kinds of functional groups onto the cage surface.³ Indeed, exohedral modification has shown great success in generating numerous functional materials, some of which have found practical use. The unusual ball-like structure of fullerenes enables another possible strategy for derivatization, i.e. endohedral doping, which has recently attracted interest for synthesis of new hybrid molecules with multiple functions.⁴ Metal atoms or metallic clusters can be encapsulated inside fullerene cavities, thereby creating endohedral metallofullerenes (EMFs). Because charge transfer takes place from metal to cage, the physicochemical properties of EMFs differ markedly from those of empty fullerenes; accordingly, they are expected to be more useful.⁵

Certainly EMFs should also be modified with different functional groups in order to make such molecules compatible in various systems.⁶ However, the chemistry of EMFs has lagged far behind that of empty fullerenes because of their low production yields. Taking advantage of high-efficiency synthesis and isolation methods developed recently, chemical modification of EMFs has blossomed a lot. Special attention has been

paid to the chemical behaviors of the high-yield $M@C_{82}$ species and the metal nitride cluster family $M_3N@C_{2n}$.⁶ Interesting results have been obtained in association with the influence of internal metals on the chemical behaviors of the cage carbons (and the whole molecules as well). For instance, the metal location and cluster size in some typical EMFs exert fundamental influences on the chemical reactivities of the whole molecules.⁷

Despite the achievements in chemical understanding of $M@C_{82}$ and $M_3N@C_{2n}$ species, little is known about the chemistry of EMFs with other contents. Metal carbide cluster EMFs (CCMFs), another important family of cluster fullerenes, have attracted much interest because of their intractable structures: two carbon atoms are encapsulated inside the cage not constructing the frame. Since the first recognition of $\text{Sc}_2\text{C}_2@D_{2d}(23)-C_{84}$, many isomers of CCMFs have been identified.⁸ It is particularly interesting and somewhat surprising that many EMFs that had been previously assigned as conventional EMFs $\text{Sc}_x@C_{2n}$ ($x = 2$ or 3 , $2n = 80, 82, 84$)⁹ have been identified recently as CCMFs $\text{Sc}_x\text{C}_2@C_{2n-2}$. Nevertheless, chemical properties of CCMFs are rarely known. Only the carbene adducts of CCMFs have been reported, but in these literatures the chemical modification is mainly utilized to ease the single-crystal growth so that no details about the reaction itself was described.^{8b,d,h} A recent report on the Prato reaction of $\text{Sc}_3\text{C}_2@C_{80}$ presented only theoretical and spectroscopic results: no X-ray structural data were reported.^{8g}

Received: November 7, 2011

Published: January 6, 2012

This article describes the reaction of $\text{Sc}_2\text{C}_2@C_{2v}(5)-C_{80}$ with 2-adamantane-2,3-[3H]-diazirine (AdN_2 , **1**) and complete characterization of the isolated monoadducts (**2a–2e**). X-ray crystallographic results of all major isomers (**2a–2c**, **2e**) and the isomerization process from the most abundant isomer (**2b**) to another one (**2c**) show that the orientation, configuration, and conformation of the internal metallic cluster are critical factors dictating the addition patterns and the relative stability of the adducts.

EXPERIMENTAL SECTION

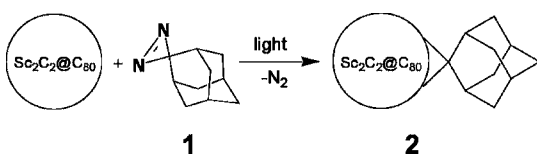
Materials and General Instruments. The EMFs were synthesized using an improved arc-discharge method and isolated with HPLC technique, as previously described.^{8h} Toluene used for reaction was distilled over sodium/benzophenone, and 1,2-dichlorobenzene used in the electrochemical measurements was distilled over P_2O_5 under argon atmosphere.

High performance liquid chromatography (HPLC) employing specific columns (Buckyprep and/or Buckyclutcher, i.d. 20 mm \times 250 mm, Nacalai Cosmosil) was conducted on a LC-908 machine (Japan Analytical Industry Co., Ltd.) with filtrated toluene as mobile phase. Matrix-assisted laser desorption/ionization time-of-flight (MALDI-TOF) mass spectrometry were measured on a BIFLEX III spectrometer (Bruker, Germany) using 1,1,4,4-tetraphenyl-1,3-butadiene as matrix. UV-vis-NIR spectra were measured on a UV 3150 spectrometer (Shimadzu, Japan) in CS_2 . Cyclic voltammogram (CV) and differential pulse voltammogram (DPV) were measured in distilled 1,2-dichlorobenzene (ODCB) with 0.1 M (*n*-Bu)₄NPF₆ at Pt working electrode with a potentiostat/galvanostat workstation (BAS CW-50). The scan rate of CV was 20 mV s⁻¹. Conditions of DPV: pulse amplitude, 50 mV; scan rate, 20 mV s⁻¹. The ¹³C NMR spectra were measured on a Bruker AVANCE 500 spectrometer with a CryoProbe system in 1,1,2,2-tetrachloroethane-*d*₂/ CS_2 (v:v = 1:4).

Geometries were optimized with hybrid density functional theory at the B3LYP level¹⁰ using the Gaussian 03 program.¹¹ The effective core potential (ECP) and (5s5p5d)/[4s4p3d] basis set were used for Sc, and the split-valence d-polarized 6-31G(d) basis set was used for C and H.¹²

Synthesis of 2. AdN_2 (**1**) was synthesized and purified according to the literature procedure.¹³ A toluene/ODCB (9:1) solution of $\text{Sc}_2\text{C}_2@C_{2v}(5)-C_{80}$ (10 mg, 9.3×10^{-4} M) and an excess amount of **1** (~30-fold) in a flask was degassed through a freeze-pump-thaw process. Then, the solution was irradiated at room temperature using a high-pressure mercury lamp with a filter cutting off the light under 350 nm (Scheme 1).¹⁵ The reaction was monitored with HPLC, and

Scheme 1. Photochemical Reaction of $\text{Sc}_2\text{C}_2@C_{2v}(5)-C_{80}$ with **1**



the profiles are shown in Figure 1. After 2 min, monoadduct peaks appeared between 12 and 15 min, and the small peaks before 10 min are from multiple adducts. Subsequent isolation with multistage preparative HPLC (Figure S1, Supporting Information) gave rise to five isolated monoadduct isomers **2a–2e** in a relative ratio of 20%, 40%, 25%, 5%, and 10%, respectively (Figure 2a).

Crystallization and XRD Characterization of 2a, 2b, 2c, and 2e. Single crystals were obtained by layering hexane over a saturated solution (dichlorobenzene/ CS_2 , v:v = 1:1) of the derivatives inside a glass tube (i.d. 7 mm). Over a period of one or two weeks, black crystalline rods formed at the bottom of the tube. X-ray data of **2a**, **2c**, and **2e** were collected at 90 K with a Bruker APEX II diffractometer equipped with a CCD collector. The crystal of **2b** was measured at

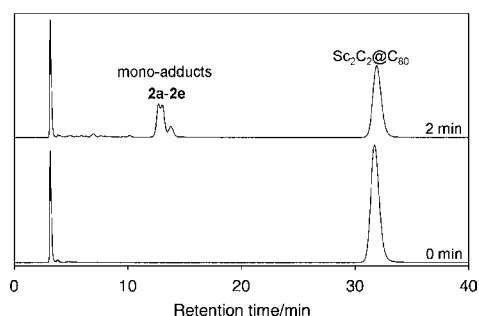


Figure 1. HPLC tracing of the reaction between $\text{Sc}_2\text{C}_2@C_{2v}(5)-C_{80}$ with **1** using a Buckyprep column.

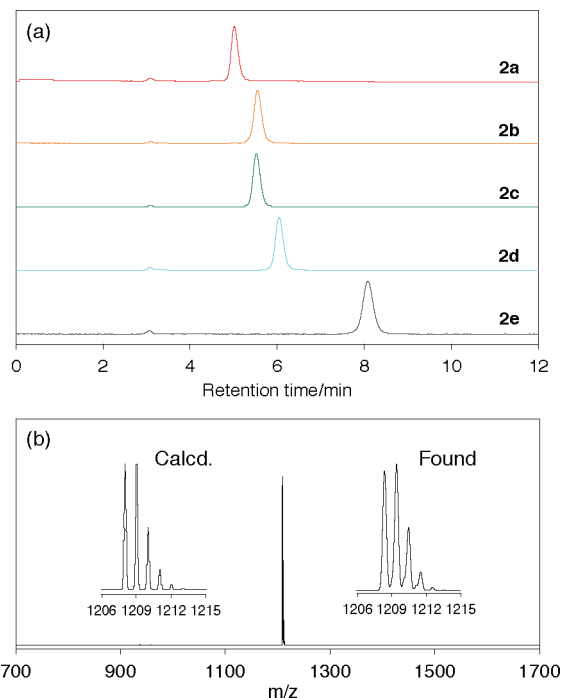


Figure 2. (a) HPLC profiles of isolated **2a–2e** using a Buckyclutcher column. (b) MALDI-TOF spectrum of **2a** in a positive reflection mode. Insets show the observed and calculated isotropic distributions.

90 K with a Rigaku DSC imaging plate system using monochromatic silicon synchrotron radiation ($\lambda = 1.00000$ Å) at beamline BL-1 A of Photon Factory (PF), High-Energy Accelerator Research Organization (KEK, Japan). Numerical methods were employed for absorption correction, and direct methods were used to solve the structures. The structures were refined using SHELX 97.¹⁴

Thermal Isomerization from 2b to 2c. A sealed glass tube containing degassed toluene solution of pure **2b** was heated at 100 °C for 48 h. After natural cooling to room temperature, the resulting mixture was examined by HPLC. Two peaks, ascribed to **2b** and **2c** in a relative ratio of 12% and 88%, respectively, were identified.

RESULTS AND DISCUSSION

Formation of the monoadducts is firmly evidenced by MALDI-TOF spectrometry. The mass spectra of **2a–2e** are essentially identical so that only the one of **2a** is presented in Figure 2b as a representative. Others are collectively shown in Figure S2, Supporting Information. Only one peak at m/z 1208 is observed which can be easily ascribed to $\text{Sc}_2\text{C}_2@C_{80}(\text{C}_{10}\text{H}_{14})$, indicating a high stability of the derivatives. Actually, Ad derivatives of EMFs reported previously were all found very stable, indicating that such materials are promising materials in

energy-conversion systems.¹⁵ Furthermore, the observed isotopic distribution agrees perfectly with the calculated one, further confirming the formation of 1:1 adducts.

Elucidation of the molecule structures of the derivatives (**2a–2e**) is certainly the first task of this work. To obtain structural information, ¹³C NMR measurements were first performed. Those of **2a**, **2b**, and **2c** (Figures S3–S6, Supporting Information) show roughly 80 lines in the aromatic region, which are from the cage, and 10 sp³ lines which are attributable to the Ad unit. This C₁ symmetry precludes further estimation of exact addition sites. The spectrum of **2e** is different, displaying 41 lines (39 full intensity + 2 half intensity) of the cage and 7 lines (3 full intensity + 4 half intensity) of the Ad group, consistent with C_s symmetry. This indicates that the Ad unit adds across one of the mirror planes of the cage. Furthermore, the signals of the C₂ unit of Sc₂C₂ are observed at 227.9, 234.9, 235.8, and 222.9 ppm for **2a**, **2b**, **2c**, and **2e**, respectively, which are almost identical to that of pristine Sc₂C₂@C_{2v}(5)-C₈₀ (231.5 ppm),^{8h} indicating that the local environments of the C₂-unit in the derivatives are mutually similar to that in the pristine.

Single crystallization was performed to accurately elucidate the structures of the derivatives. High-quality single crystals of all the abundant isomers (**2a**, **2b**, **2c**, and **2e**) were obtained, and all were found suitable for XRD measurements and further structural analyses. Their molecular structures are unambiguously established.

In all crystals, the Ad group is perfectly ordered, but both the cage and the internal cluster show some degree of disorder except **2e** which shows no cluster disorder, and its two cage orientations only shift a little from each other. During the refinements, the cage, the C₂-unit, and the metal atoms are all refined independently. The X-ray structures of **2a**, **2b**, **2c**, and **2e** with all disordered components are shown in Figure S10, Supporting Information. Figure 3 illustrates the structures with

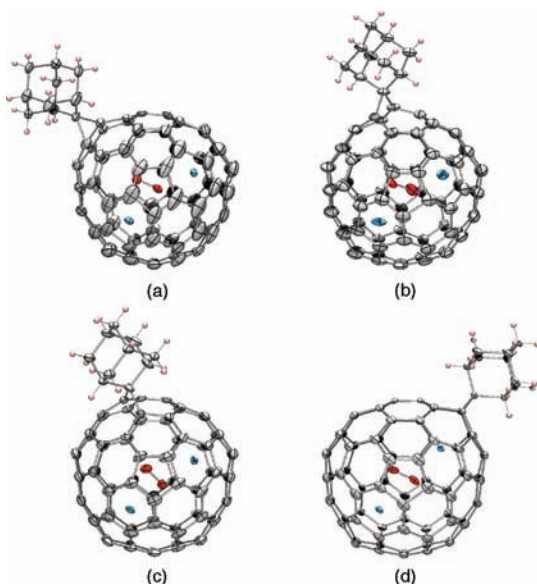


Figure 3. ORTEP drawings of (a) **2a**, (b) **2b**, (c) **2c**, (d) **2e**, showing thermal ellipsoids at the 50% probability level. All show the same cage orientation. Solvent molecules are omitted for clarity, and only the major sites of the cage and the cluster are shown. Sc(1) and Sc(2) mentioned in the text correspond to the upper and the lower metal atoms, respectively.

only the major cage and the major cluster, in which all cages show the same orientation to ease comparison.

The crystal unit of **2a** contains a whole cage with two disordered orientations showing respective population of 0.54 and 0.46, which are mutual enantiomers. The unit cavity is filled with several disordered solvent molecules such as 1,2-dichlorobenzene (ODCB) and CS₂. For the internal cluster, two sets of C₂-unit with respective occupancies of 0.71 and 0.29 are distinguished, but as many as 10 positions of the two Sc atoms are readily observed. Considering their stereo relations and matching occupancies, some Sc positions can be paired with one of the two C₂-unit orientations. This result indicates that the two metals are hopping inside the cage, but the motion of the C₂-unit is largely hindered.

Figure 3a shows the molecular structure of **2a** with the major cage (0.54), the major C₂-unit (0.71) and two of the major Sc atoms (0.33 for Sc1 and 0.31 for Sc2). Ad adds to a [6,6]-bond junction abutted by two pentagons which is remote from either Sc atom. The distance between the carbon atoms at the site of addition (1.58 Å) suggests a closed-cage structure rather than an open cage, which is also consistent with the NMR results presenting a sp³ signal at 67.26 ppm (Figure S3, Supporting Information). This result is somewhat surprising because all other EMF-Ad derivatives, including **2b**, **2c**, and **2e** (see below), have open-cage structures.¹⁵ It is still difficult to give any prediction or explanation about whether the adduct is open or closed at the present stage of research because of insufficient experimental and theoretical results.

Also two enantiomeric cage orientations are found in **2b**, with respective ratio of 0.72 and 0.28. Two C₂-unit orientations are confirmed to have 0.54 and 0.46 occupancy values, respectively, along with eight Sc positions. These results confirm again that the metals are hopping inside the cage, whereas the C₂-unit is almost fixed. Severely disordered solvent molecules (ODCB) reduce the quality of crystal. Figure 3b shows the molecular structure of **2b** with the major cage (0.72), the major C₂-unit (0.54), and the two major Sc atoms (0.58 for Sc1 and 0.57 for Sc2). Ad breaks a [5,6]-bond on the cage remote from either Sc atom. The C–C distance between the carbons at the site of addition is 1.97 Å, corresponding to an open-cage structure.

The situation in **2c** is very similar to those in the previous two cases: two cage orientations (0.52 and 0.48, respectively), two C₂-unit orientations (0.53 and 0.47, respectively), and eight Sc positions are apparent, showing a carbide cluster with two moving metals around a steady C₂-unit core. Figure 3c shows the molecular structure of **2c** consisting of the major components. A [6,6]-bond is broken by the addition of Ad, and the relatively long distance (1.76 Å) between the cage carbons at the site of addition indicates an open cage rather than a closed structure. It is noteworthy that the Ad group shares a common cage carbon in **2b** and **2c**, although this results respectively in [5,6]- and [6,6]-adducts, which makes possible an isomerization process from **2b** to **2c** (vide infra).

Structure of **2e** is rather different, as already reported.^{8h} only one set of Sc₂C₂ is observed together with two disordered cage orientations (0.57 and 0.43), which mutually shift by ~0.5 Å. From the illustration shown in Figure 3d which shows only the major cage, Ad breaks a [6,6]-bond across one of the mirror planes of the cage, resulting in a C_s-symmetric molecule. The distance of carbons at the site of addition is 2.13 Å, unambiguously confirming an open-cage structure. These X-ray data show perfect agreement with the ¹³C NMR results. It is noteworthy that the addition sites in **2e** is close to one of the two Sc atoms, and resulting a situation that the metal nearby is trapped inside the cavity of the broken bond and the cluster is

more planar. This could also be the reason that in **2e** the cluster are fixed, rather than hopping.

It is noteworthy that although several metal positions are distinguished in most cases (**2a–2c**), the stereo relations between the C_2 -unit and the cage are very similar among these isomers (Figure 3). Furthermore, our calculations (Figure S7, Supporting Information) show that the most stable structure of pristine $Sc_2C_2@C_{2v}(5)-C_{80}$ has the same cluster orientation as those of **2a**, **2b**, and **2c** shown in Figure 3. In addition, the C–C bond lengths of the C_2 -unit in the cluster are not affected by the addition to different sites. The values in **2a–2c** are almost equal (1.169–1.18 Å), which is only 0.053 Å shorter than that in **2e** (1.222 Å) at most. Considering the similar NMR values of the C_2 -unit in the pristine and the derivatives, it appears conclusive that these two carbons bond very tightly, avoiding any possible interaction with the cage carbons. These results are helpful to explain the fact that Sc-EMFs with two or more metals reported so far are mostly cluster species; the strong coordination ability of Sc (and also other rare earth metals) favors the formation of various clusters, and the small ionic radius of Sc permits the encapsulation of these clusters inside medium-sized fullerenes (e.g., C_{80} – C_{84}).¹⁶ This conclusion adds a new concept to the formation mechanism of EMFs, especially cluster EMFs.

The addition patterns in **2a**, **2b**, **2c**, and **2e** disclosed by XRD are not explainable by just considering the strain and charge on the cage carbons, although this strategy has previously shown great success in elucidating the addition patterns in $M@C_{2v}-C_{82}$ and even in the non-IPR $La_2@D_2(10611)-C_{72}$.¹⁵ When considering a fixed cluster with lowest energy for the whole molecule, the negative charges and bond strains are mainly localized on the cage carbons near the two metals, which is easy to understand because the positively charged metal ions attract high negative charges onto the nearby carbons and the bending cluster extrudes the cage parts near the metals. However, the addition positions in **2a–2c** are all far from the major orientations of the two Sc atoms (Figure 3), where relatively low POAV angles and charge density values are localized (Figure S8, Supporting Information). Obviously, this strategy is no longer effective to explain the situations in **2a–2c**, although it is fairly intuitive for the circumstances in **2e** with a relative abundance of only 10%.

We have reported that the internal cluster in $Sc_2C_2@C_{2v}(5)-C_{80}$ is not always fixed inside the cage. When the temperature is higher than 373 K, the cluster is rotating.^{8h} Although the reaction under study is performed at room temperature (298 K) and the irradiation time is very short (2 min), the energy from the light may have rotated or orientated the cluster in a different manner from the one lowest in energy. Accordingly, the addition patterns in **2a–2e** may result from cluster rotation under irradiation. On the other hand, we found that the addition patterns in **2a–2e** might be partially explained by the frontier molecular orbital theory considerations. As Figure 4 shows, although HOMOs of $Sc_2C_2@C_{2v}(5)-C_{80}$ mostly distribute over the region under the arch of the cluster, LUMOs spread mainly over the surface on top of the cluster arch and molecular orbital could find large coefficients on these carbons of addition in **2a**, **2b**, and **2c**. Nevertheless, the circumstances in CCMFs are obviously more complicated than these in conventional EMFs and the nitride cluster family. Future investigations are still necessary to make the mechanism clearer.

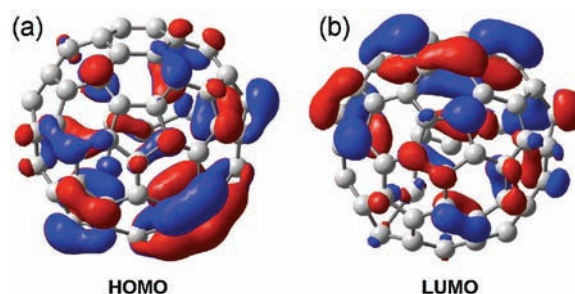


Figure 4. (a) HOMO and (b) LUMO of $Sc_2C_2@C_{2v}(5)-C_{80}$. Both show the same cage orientation as those in Figure 3.

Figure 5 shows the vis–NIR spectra of $Sc_2C_2@C_{2v}(5)-C_{80}$ and its derivatives **2a–2e**. The lines are roughly similar but

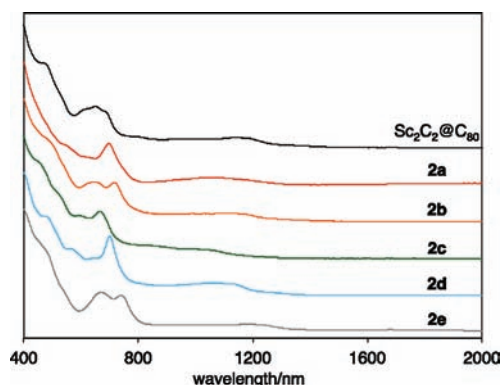


Figure 5. Vis–NIR spectra of pristine $Sc_2C_2@C_{2v}(5)-C_{80}$ and **2**.

differences are visible among the distinct absorptions between 600 and 800 nm, as well as the optical onsets. Because cluster orientations in these derivatives are roughly similar (Figure 3) or the cluster is rotating, these optical differences among **2a–2e** and pristine $Sc_2C_2@C_{2v}(5)-C_{80}$ may originate from the different addition sites. This indicates that their electronic structures are mainly cage-based.

Electrochemical behaviors of $Sc_2C_2@C_{2v}(5)-C_{80}$ and **2a–2e** were also investigated. The redox potentials are presented in Table 1. It is evident that corresponding values of **2a–2e** are

Table 1. Redox Potentials (V vs Fc^+/Fc) of $Sc_2C_2@C_{2v}(5)-C_{80}$ and **2a–2e**^a

| compd | ^{ox} E_1 | ^{red} E_1 | ^{red} E_2 |
|------------------|---------------------|----------------------|----------------------|
| $Sc_2C_2@C_{80}$ | 0.41 | −0.74 | −1.33 |
| 2a | 0.14 | −0.96 | −1.69 |
| 2b | 0.28 | −0.87 | −1.56 |
| 2c | 0.27 | −0.89 | −1.48 |
| 2d | 0.28 | −0.86 | −1.53 |
| 2e | 0.11 | −0.75 | −1.46 |

^aHalf-cell potentials unless otherwise noted. Values were obtained at a Pt working electrode in a 1,2-dichlorobenzene solution containing 0.1 M (*n*-Bu)₄NPF₆.

cathodically shifted by 0.01–0.30 V as compared with those of pristine $Sc_2C_2@C_{2v}(5)-C_{80}$, indicating a mild electron-donating ability of Ad. This is consistent with previous observations, and the results are certainly useful to future works making EMF derivatives as photovoltaic materials.¹⁵

Isomerization from 2b to 2c. An interesting isomerization process from **2b** to **2c** was observed during the experiments examining thermal stabilities of **2a–2e**. All isomers are thermally stable except **2b** which isomerizes into **2c** under heating. As shown in Figure 6, HPLC results confirm that the

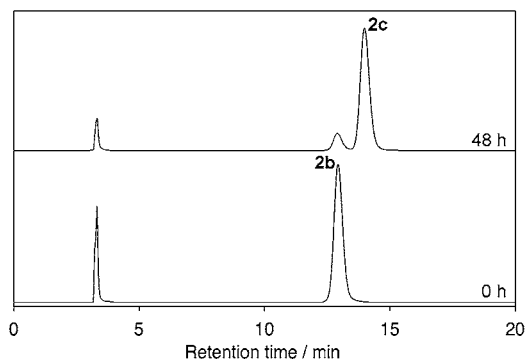


Figure 6. Tracing isomerization from **2b** to **2c** with HPLC.

heated solution of **2b** exhibits two peaks, which are ascribed to **2b** (12%) and **2c** (88%) according to their absorption spectra. More interestingly, the isomerization also proceeds in solid state: the crystal of **2b** gradually changed to that of **2c** at room temperature over a period of one year as confirmed by X-ray crystallography. This is also a main reason for the low crystal quality of **2b**. Because **2b** and **2c** share a common cage carbon (cf. Figure 3), the isomerization most probably follows the ‘pirouette’ rearrangement process.¹⁷ DFT calculations show that **2b** is 14.82 kcal/mol higher in energy than **2c**, confirming that **2b** is only a kinetically favorable adduct.

CONCLUSION

Reaction of a new carbide cluster EMF, $\text{Sc}_2\text{C}_2@C_{2v}(5)-C_{80}$ with adamantylidene carbene (**1**) affords five isolable mono-adduct isomers whose structures and properties are fully characterized. Concrete single-crystal XRD crystallographic results of all major isomers reveal that the addition mostly takes place at a cage region on top of the arch of the cluster, and after functionalization, the two Sc atoms are more likely to move although the C_2 -unit is almost fixed relative to the cage. Such addition patterns most probably result from a rotating cluster and are partially explainable by considering the molecular orbital distributions on the cage surface. Although the Sc atoms are obviously affected by the addition, the C–C distance within the carbide cluster remains nearly constant in all isomers. However, the electronic structures of the derivatives are very sensitive to the addition sites, and the Ad group has an electron-donating effect on the cage. Our results have provided new insights into the chemical properties of CCMFs. They are expected to stimulate more studies that will eventually clarify the mysteries in such little-investigated species.

ASSOCIATED CONTENT

Supporting Information

Complete citation of references 11, 15a, 15b, HPLC separation profiles, NMR spectra, summary of ¹³C NMR chemical shifts, calculated results of $\text{Sc}_2\text{C}_2@C_{2v}(5)-C_{80}$, and X-ray data of $\text{Sc}_2\text{C}_2@C_{2v}(5)-C_{80}\text{Ad}$ (**2a**, **2b**, **2c**, **2e**). This material is available free of charge via the Internet at <http://pubs.acs.org>.

AUTHOR INFORMATION

Corresponding Author

akasaka@tara.tsukuba.ac.jp; nagase@ims.ac.jp

ACKNOWLEDGMENTS

This work is supported in part by a Grant-in-Aid for Scientific Research on Innovative Areas (No. 20108001, “pi-Space”), a Grant-in-Aid for Scientific Research (A) (No. 20245006), The Next Generation Super Computing Project (Nanoscience Project), Nanotechnology Support Project, and a Grant-in-Aid for Scientific Research on Priority Area (Nos. 20036008, 20038007) and Specially Promoted Research from the Ministry of Education, Culture, Sports, Science, and Technology of Japan. H.K. thanks the Japan Society for the Promotion of Science (JSPS) for the Research Fellowship for Young Scientists.

REFERENCES

- (1) (a) Geim, A. K.; Novoselov, K. S. *Nat. Mater.* **2007**, *6*, 183–191. (b) Allen, M. J.; Tung, V. C.; Kaner, R. B. *Chem. Rev.* **2010**, *110*, 132–145. (c) Vostrowsky, O.; Hirsch, A. *Angew. Chem., Int. Ed.* **2004**, *43*, 2326–2329. (d) Fowler, P. W.; Manolopoulos, D. E. *An Atlas of Fullerenes*; Oxford Press: Clarendon, 1995.
- (2) (a) Thilgen, C.; Diederich, F. *Chem. Rev.* **2006**, *106*, 5049–5135. (b) *Fullerenes: Recent Advances in the Chemistry and Physics of Fullerenes and Related Materials*; Kadish, K. M.; Ruoff, R. S., Eds.; The Electrochemical Society, Pennington, NJ, 1997. (c) Nakamura, E.; Isobe, H. *Chem. Rev.* **2010**, *10*, 260–270.
- (3) (a) Hirsch, A.; Brettreich, M. *Fullerenes: Chemistry and Reactions*; Wiley-VCH, 2005. (b) Giacalone, F.; Martin, N. *Chem. Rev.* **2006**, *106*, 5136–5190. (c) Matsuo, Y.; Nakamura, E. *Chem. Rev.* **2008**, *108*, 3016–3028.
- (4) (a) *Endofullerenes: A New Family of Carbon Clusters*, Akasaka, T., Nagase, S., Eds.; Kluwer: Dordrecht, The Netherlands, 2002. (b) *Chemistry of Nanocarbons*; Akasaka, T., Wudl, F., Nagase, S., Eds.; Wiley-Blackwell: London, 2010. (c) Lu, X.; Akasaka, T.; Nagase, S. *Rare Earth Metals Trapped inside Fullerenes: Endohedral Metallofullerenes, in Rare Earth Coordination Chemistry: Fundamentals and Applications*; Huang, C. H., Ed.; John Wiley & Sons: Singapore, 2010; pp 273–308.
- (5) (a) Chaur, M. N.; Melin, F.; Ortiz, A. L.; Echegoyen, L. *Angew. Chem., Int. Ed.* **2009**, *48*, 7514–7538. (b) Yamada, M.; Akasaka, T.; Nagase, S. *Acc. Chem. Res.* **2010**, *43*, 92–102. (c) Dunsch, L.; Yang, S. *Small* **2007**, *3*, 1298–1320. (d) Rodriguez-Fortea, A.; Balch, A. L.; Poblet, J. M. *Chem. Soc. Rev.* **2011**, *40*, 3551–3563.
- (6) (a) Lu, X.; Akasaka, T.; Nagase, S. *Chem. Commun.* **2011**, *47*, 5942–5957. (b) Maeda, Y.; Tsuchiya, T.; Lu, X.; Takano, Y.; Akasaka, T.; Nagase, S. *Nanoscale* **2011**, *3*, 2421–2429. (c) Osuna, S.; Swart, M.; Sola, M. *Phys. Chem. Chem. Phys.* **2011**, *13*, 3585–3603.
- (7) (a) Lu, X.; Nikawa, H.; Feng, L.; Tsuchiya, T.; Maeda, Y.; Akasaka, T.; Mizorogi, N.; Slanina, Z.; Nagase, S. *J. Am. Chem. Soc.* **2009**, *131*, 12066–12067. (b) Lu, X.; Nikawa, H.; Tsuchiya, T.; Akasaka, T.; Toki, M.; Sawa, H.; Mizorogi, N.; Nagase, S. *Angew. Chem., Int. Ed.* **2010**, *49*, 594–597. (c) Lukoyanova, O.; Cardona, C. M.; Rivera, J.; Lugo-Morales, L. Z.; Chancellor, C. J.; Olmstead, M. M.; Rodriguez-Fortea, A.; Poblet, J. M.; Balch, A. L.; Echegoyen, L. *J. Am. Chem. Soc.* **2007**, *129*, 10423–10430. (d) Cardona, C. M.; Elliott, B.; Echegoyen, L. *J. Am. Chem. Soc.* **2006**, *128*, 6480–6485.
- (8) (a) Wang, C. R.; Kai, T.; Tomiyama, T.; Yoshida, T.; Kobayashi, Y.; Nishibori, E.; Takata, M.; Sakata, M.; Shinohara, H. *Angew. Chem., Int. Ed.* **2001**, *40*, 397–399. (b) Iiduka, Y.; Wakahara, T.; Nakahodo, T.; Tsuchiya, T.; Sakuraba, A.; Maeda, Y.; Akasaka, T.; Yoza, K.; Horn, E.; Kato, T.; Liu, M. T. H.; Mizorogi, N.; Kobayashi, K.; Nagase, S. *J. Am. Chem. Soc.* **2005**, *127*, 12500–12501. (c) Iiduka, Y.; Wakahara, T.; Nakajima, K.; Tsuchiya, T.; Nakahodo, T.; Maeda, Y.; Akasaka, T.; Mizorogi, N.; Nagase, S. *Chem. Commun.* **2006**, 2057–2059. (d) Iiduka, Y.; Wakahara, T.; Nakajima, K.; Nakahodo, T.; Tsuchiya, T.; Maeda, Y.;

Akasaka, T.; Yoza, K.; Liu, M. T. H.; Mizorogi, N.; Nagase, S. *Angew. Chem., Int. Ed.* **2007**, *46*, 5562–5564. (e) Yamazaki, Y.; Nakajima, K.; Wakahara, T.; Tsuchiya, T.; Ishitsuka, M. O.; Maeda, Y.; Akasaka, T.; Waelchli, M.; Mizorogi, N.; Nagase, S. *Angew. Chem., Int. Ed.* **2008**, *47*, 7905–7908. (f) Wang, T. S.; Chen, N.; Xiang, J. F.; Li, B.; Wu, J. Y.; Xu, W.; Jiang, L.; Tan, K.; Shu, C. Y.; Lu, X.; Wang, C. R. *J. Am. Chem. Soc.* **2009**, *131*, 16646–16647. (g) Wang, T. S.; Wu, J. Y.; Xu, W.; Xiang, J. F.; Lu, X.; Li, B.; Jiang, L.; Shu, C. Y.; Wang, C. R. *Angew. Chem., Int. Ed.* **2010**, *49*, 1786–1789. (h) Kurihara, H.; Lu, X.; Iiduka, Y.; Mizorogi, N.; Slanina, Z.; Tsuchiya, T.; Akasaka, T.; Nagase, S. *J. Am. Chem. Soc.* **2011**, *133*, 2382–2385. (i) Lu, X.; Nakajima, K.; Iiduka, Y.; Nikawa, H.; Mizorogi, N.; Slanina, Z.; Tsuchiya, T.; Nagase, S.; Akasaka, T. *J. Am. Chem. Soc.* **2011**, *133*, 19553–19558.

(9) (a) Takata, M.; Nishibori, E.; Sakata, M.; Inakuma, M.; Yamamoto, E.; Shinohara, H. *Phys. Rev. Lett.* **1999**, *83*, 2214–2217. (b) Takata, M.; Nishibori, E.; Umeda, B.; Sakata, M.; Yamamoto, E.; Shinohara, H. *Phys. Rev. Lett.* **1997**, *78*, 3330–3333. (c) Inakuma, M.; Yamamoto, E.; Kai, T.; Wang, C. R.; Tomiyama, T.; Shinohara, H.; Dennis, T. J. S.; Hulman, M.; Krause, M.; Kuzmany, H. *J. Phys. Chem. B* **2000**, *104*, 5072–5077.

(10) (a) Becke, A. D. *Phys. Rev. A* **1988**, *38*, 3098–3100. (b) Becke, A. D. *J. Chem. Phys.* **1993**, *98*, 5648–5652. (c) Lee, C.; Yang, W.; Parr, R. G. *Phys. Rev. B* **1988**, *37*, 785–789.

(11) Frisch, M. J. et al. *Gaussian 03*, Revision C. 01; Gaussian Inc.: Wallingford, CT, 2004.

(12) (a) Hay, P. J.; Wadt, W. R. *J. Chem. Phys.* **1985**, *82*, 299–310. (b) Francl, M. M.; Pietro, W. J.; Hehre, W. J.; Binkley, J. S.; Gordon, M. S.; DeFrees, D. J.; Pople, J. A. *J. Chem. Phys.* **1982**, *77*, 3654–3665.

(13) Antonio, R. F.; Campanera, M. J.; Cardona, C. M.; Echegoyen, L.; Polet, J. M. *Angew. Chem., Int. Ed.* **2006**, *45*, 8176.

(14) Sheldrick, G. M. *Acta Crystallogr.* **2008**, *A64*, 112–122.

(15) (a) Maeda, Y.; et al. *J. Am. Chem. Soc.* **2004**, *126*, 6858–6859.

(b) Akasaka, T.; et al. *J. Am. Chem. Soc.* **2008**, *130*, 12840–12841.

(c) Takano, Y.; Aoyagi, M.; Yamada, M.; Nikawa, H.; Slanina, Z.; Mizorogi, N.; Ishitsuka, M. O.; Tsuchiya, T.; Maeda, Y.; Akasaka, T.; Kato, T.; Nagase, S. *J. Am. Chem. Soc.* **2009**, *131*, 9340–9346. (d) Lu, X.; Nikawa, H.; Nakahodo, T.; Tsuchiya, T.; Ishitsuka, M. O.; Maeda, Y.; Akasaka, T.; Toki, M.; Sawa, H.; Slanina, Z.; Mizorogi, N.; Nagase, S. *J. Am. Chem. Soc.* **2008**, *130*, 9129–9136. (e) Lu, X.; Nikawa, H.; Tsuchiya, T.; Maeda, Y.; Ishitsuka, M. O.; Akasaka, T.; Toki, M.; Sawa, H.; Slanina, Z.; Mizorogi, N.; Nagase, S. *Angew. Chem., Int. Ed.* **2008**, *47*, 8642–8645.

(16) (a) Zuo, T. M.; Beavers, C. M.; Duchamp, J. C.; Campbell, A.; Dorn, H. C.; Olmstead, M. M.; Balch, A. L. *J. Am. Chem. Soc.* **2007**, *129*, 2035–2043. (b) Lu, X.; Lian, Y.; Beavers, C. M.; Mizorogi, N.; Slanina, Z.; Nagase, S.; Akasaka, T. *J. Am. Chem. Soc.* **2011**, *133*, 10772–10775.

(17) (a) Cai, T.; Slobodnick, C.; Xu, L.; Harich, K.; Glass, T. E.; Chancellor, C.; Fetting, J. C.; Olmstead, M. M.; Balch, A. L.; Gibson, H. W.; Dorn, H. C. *J. Am. Chem. Soc.* **2006**, *128*, 6486–6492.

(b) Cardona, C. M.; Kitaygorodskiy, A.; Echegoyen, L. *J. Am. Chem. Soc.* **2005**, *127*, 10448–10453. (c) Takano, Y.; Ishitsuka, M. O.; Tsuchiya, T.; Akasaka, T.; Kato, T.; Nagase, S. *Chem. Commun.* **2010**, *46*, 8035–8036. (d) Lu, X.; Nikawa, H.; Kikuchi, T.; Mizorogi, N.; Slanina, Z.; Tsuchiya, T.; Nagase, S.; Akasaka, T. *Angew. Chem., Int. Ed.* **2011**, *50*, 6356–6359.